eBioscience
Accelerate Your Research
view details
Receive a FREE iPad3 with qualifying order

THE JOURNAL OF IMMUNOLOGY

This information is current as of June 4, 2012.

The Aryl Hydrocarbon Receptor Modulates Acute and Late Mast Cell Responses

Riccardo Sibilano, Barbara Frossi, Marco Calvaruso, Luca Danelli, Elena Betto, Alessandra Dall'Agnese, Claudio Tripodo, Mario P. Colombo, Carlo E. Pucillo and Giorgia Gri

J Immunol published online 30 May 2012
http://www.jimmunol.org/content/early/2012/05/30/jimmunol.1200009

Supplementary Material http://www.jimmunol.org/content/suppl/2012/05/30/jimmunol.1200009.DC1.html

Subscriptions Information about subscribing to *The Journal of Immunology* is online at: http://jimmunol.org/subscriptions

Permissions Submit copyright permission requests at: http://www.aai.org/ji/copyright.html

Email Alerts Receive free email-alerts when new articles cite this article. Sign up at: http://jimmunol.org/cgi/alerts/etoc

The Journal of Immunology is published twice each month by
The American Association of Immunologists, Inc.,
9650 Rockville Pike, Bethesda, MD 20814-3994.
Copyright © 2012 by The American Association of Immunologists, Inc. All rights reserved.
Print ISSN: 0022-1767 Online ISSN: 1550-6606.

Downloaded from http://jimmunol.org/ at Inst Superiore de Sanita-Roma on June 4, 2012

Published May 30, 2012, doi:10.4049/jimmunol.1200009

The Aryl Hydrocarbon Receptor Modulates Acute and Late Mast Cell Responses

Riccardo Sibilano,*,[1] Barbara Frossi,* Marco Calvaruso,† Luca Danelli,* Elena Betto,* Alessandra Dall'Agnese,* Claudio Tripodo,† Mario P. Colombo,‡ Carlo E. Pucillo,* and Giorgia Gri*

The aryl hydrocarbon receptor (AhR) is a ligand-dependent transcription factor whose activity is modulated by xenobiotics as well as physiological ligands. These compounds may modulate inflammatory responses and contribute to the rising prevalence of allergic diseases observed in industrialized countries. Mast cells (MCs), located within tissues at the boundary of the external environment, represent a potential target of AhR ligands. In this study, we report that murine and human MCs constitutively express AhR, and its activation by the high-affinity ligand 6-formylindolo[3,2-*b*]carbazole (FICZ) determines a boost in degranulation. On the contrary, repeated exposure to FICZ inhibits MC degranulation. Accordingly, histamine release, in an in vivo passive systemic anaphylactic model, is exacerbated by a single dose and is attenuated by repetitive stimulation of AhR. FICZ-exposed MCs produce reactive oxygen species and IL-6 in response to cAMP-dependent signals. Moreover, AhR-activated MCs produce IL-17, a critical player in chronic inflammation and autoimmunity, suggesting a novel pathway for MC activation in the pathogenesis of these diseases. Indeed, histological analysis of patients with chronic obstructive pulmonary disease revealed an enrichment in AhR/IL-6 and AhR/IL-17 double-positive MCs within bronchial lamina propria. Thus, tissue-resident MCs could translate external chemical challenges through AhR by modulating allergic responses and contributing to the generation of inflammation-related diseases. ***The Journal of Immunology*****, 2012, 188: 000–000.**

The aryl hydrocarbon receptor (AhR) is a member of the basic helix-loop-helix-Per-Arnt-Sim transcriptional factor family known to respond to environmental toxins, such as dioxin, dioxin-like compounds, and benzopyrene found in cigarette smoke, as well as to endogenous compounds, including dietary components, heme metabolites, indigoids, and tryptophan metabolites. The binding to its agonist allows AhR nuclear translocation and regulation of a large number of target genes containing dioxin responsive elements on their enhancer sequences (1). Recent data demonstrate that AhR influences immune responses and is involved in inflammatory diseases, such as experimental autoimmune encephalomyelitis (2), inflammatory bowel disease (3), and inflammatory response to cigarette smoke (4). Several groups have shown that AhR activation contributes to IL-17–producing T cell (Th17) differentiation (5), whereas others have reported that it induces natural $CD4^+CD25^+Foxp3^+$ regulatory T (Treg) cells and IL-10–producing Tr1 cells (6). Thus, the role of AhR in driving a pro- or an anti-inflammatory response is still debated. Depending on AhR agonists and the model of pathology considered, AhR may worsen or ameliorate the disease (7).

Innate immune cells, which are specifically located at the interface between host and external environment and play important roles in detoxification and protection from injury, may mediate the immunological effects of AhR modulation in vivo. Among others, mast cells (MCs) have been indicated as potent linkers between innate and adaptive immunity because of their capacity to selectively secrete cytokines and chemokines in response to a wide array of stimuli and for their ability to regulate several physiological and pathological immune responses (8). Additionally, we and others have shown that MCs are precious allies of Treg cells in arranging the tissue-restricted immune response, but their action may lead both to tolerance or inflammation, depending on the molecular milieu regulating Treg and effector T cells skewing into Th17 cells (9). Therefore, AhR expression and its possible role in modulating MC functions may have significant implications for the outcome of inflammatory pathologies where effector T cell/Treg cell balance is compromised. Interestingly, a recent study shows that the activation of AhR suppresses the development of Th2-mediated food allergic response by inducing Treg cell skewing (10). However, these data do not exclude that AhR engagement could directly affect the function of allergy effector cells, namely MCs, beyond T cells. Moreover, increasing evidence suggests alterations in MC populations in patients with chronic obstructive pulmonary disease (COPD), a chronic inflammatory disease mostly associated with cigarette smoking in which innate and

*Department of Medical and Biological Sciences, University of Udine, 33100 Udine, Italy; †Department of Human Pathology, University of Palermo, 90127 Palermo, Italy; and ‡Dipartimento di Oncologia Sperimentale e Medicina Molecolare, Fondazione Istituto di Ricovero e Cura a Carattere Scientifico "Istituto Nazionale dei Tumori," 20133 Milan, Italy

[1]Current address: Department of Pathology, Stanford University School of Medicine, Stanford, CA.

Received for publication January 3, 2012. Accepted for publication April 19, 2012.

This work was supported by grants from the Associazione Italiana Ricerca sul Cancro; Progetti di Ricerca di Interesse Nazionale from Ministero dell'Istruzione, Università e Ricerca; the Agenzia Spaziale Italiana (Osteoporosis and Muscular Atrophy Project); the Legge Regionale 11 Friuli Venezia Giulia; Fondazione Cariplo, Milan; and the Italian Ministry of Health, Labor and Social Welfare: 5% donations under the Istituto Nazionale Tumori Scientific Directorate's Special Project on Lung Cancer.

Address correspondence and reprint requests to Prof. Carlo Pucillo, University of Udine, Piazzale Massimiliano Kolbe 4, 33100 Udine, Italy. E-mail address: carlo.pucillo@uniud.it

The online version of this article contains supplemental material.

Abbreviations used in this article: AhR, aryl hydrocarbon receptor; BMMC, bone marrow-derived mast cell; CM-H_2DCFDA, 5-(and-6)-chloromethyl-2′,7′-dichlorodihydrofluorescein diacetate acetyl ester; COPD, chronic obstructive pulmonary disease; FICZ, 6-formylindolo[3,2-*b*]carbazole; MC, mast cell; NAC, *N*-acetyl-L-cysteine; PKA, protein kinase A; ROS, reactive oxygen species; Treg, regulatory T; WT, wild-type.

Copyright © 2012 by The American Association of Immunologists, Inc. 0022-1767/12/$16.00

Downloaded from http://jimmunol.org/ at Inst Superiore de Sanita-Roma on June 4, 2012

adaptive immune cells infiltrate and damage the bronchial mucosa (11). Macrophages, neutrophils, and their proteolytic mediators are involved in the extracellular matrix destruction, whereas $CD8^+$ cytotoxic T cells and Th1 and Th17 cells produce proinflammatory cytokines and promote accumulation of inflammatory cells in the lungs. As COPD progresses to its severe stages, the MC population in the lung changes its density, distribution, and phenotype (12), possibly becoming relevant to the worsening of COPD. Because the mechanisms by which lung MCs from COPD patients are activated and because MC-specific contributions to the inflammatory milieu have not yet been characterized, we speculate that the wide availability of AhR agonists in the lungs of these patients could be responsible to promote MC activation.

In this study, we investigate the functional expression of AhR in murine and human MCs discerning between early and late responses. Early MC degranulation upon Ag-specific IgE cross-linking in the presence of the AhR agonist 6-formylindolo[3,2-*b*]carbazole (FICZ) and the possible mechanism of action are dissected. To resemble the conceivable pathways of AhR ligand exposure, MCs are treated with acute or repetitive schedules of FICZ administration, revealing different behaviors.

Late IL-6 and IL-17 proinflammatory cytokine production upon FICZ exposure are monitored from bone marrow-derived mast cells (BMMCs) and human MC lines in vitro. Tissue resident MCs from bronchial mucosa of COPD patients are analyzed for AhR, IL-6, and IL-17 concomitant expression to verify MC potential to respond to smoke-containing AhR ligands.

Materials and Methods

Mice, cell lines, and reagents

C57BL/6 mice were purchased from The Jackson Laboratory and used in accordance with the National Institutes of Health Guidelines and Use Committee. AhR-deficient ($AhR^{-/-}$) mice were provided by Dr. Frank Gonzalez (National Cancer Institute, Bethesda, MD). Human MC line HMC-1 was cultured in RPMI 1640 medium supplemented with 10% FCS, 1.2 mM monothioglycerol, 100 U/ml penicillin, 100 μg/ml streptomycin, and 2 mM glutamine. Human LAD2 MC cell line was provided by Dr. Arnold Kirshenbaum (National Institutes of Health) and grown in serum-free StemPro-34 medium (Invitrogen, Carlsbad, CA) in the presence of 100 ng/ml human stem cell factor (PeproTech, London, U.K.). Human liver carcinoma cell line HepG2 was cultured in RPMI 1640 medium supplemented with 10% FBS.

DNP-specific IgE was produced as described (13). DNP human serum albumin (DNP36-HSA, Ag) and *N*-acetyl-L-cysteine (NAC) were purchased from Sigma-Aldrich (St. Louis, MO). The 6-formylindolo[3,2-b]carbazole (FICZ) was purchased from Enzo Life Sciences (Farmingdale, NY). Protein kinase A (PKA) inhibitor adenosine 3′,5′-cyclic monophosphorothioate, Rp-isomer, triethylammonium salt (Rp-cAMP), and proteasome inhibitor MG-132 were from Calbiochem (Merck, Darmstadt, Germany).

BMMC differentiation and activation

C57BL/6 murine BMMCs were obtained from in vitro differentiation of bone marrow precursors as reported in Gri et al.(14). BMMCs (2×10^6/ml) sensitized for 3 h with 1 μg/ml DNP-specific IgE were challenged in Tyrode's buffer with 50 ng/ml Ag.

Real-time PCR

RNA was isolated using TRIzol reagent (Life Technologies, Carlsbad, CA) according to the manufacturer's instructions. RNA (1 μg) was reverse-transcribed using an iScript cDNA synthesis kit (Bio-Rad, Hercules, CA). Murine *ahr* (forward, 5′-ATGGCTTTGTGCTGGGTTGTCACAG-3′; reverse, 5′-ACTCCTTGTGCAGAGTCTGGGTTT-3′) and murine *g3pdh* (forward, 5′-TCAACAGCAACTCCCACTCTTCCA-3′; reverse, 5′-ACCCTGTTGCTGTAGCCGTATTCA-3′) were synthesized and purified by MWG (Ebersberg, Germany). Real-time PCR was conducted using iQ SYBR Green Supermix (Bio-Rad), according to manufacturer's instructions in CFX96 real-time system and analyzing data with CFX Manager software (Bio-Rad). The fluorescent signals were collected during extension phase, Ct values of the sample were calculated, and the transcript levels were analyzed by the $2^{-\Delta\Delta Ct}$ method.

In vitro T cell differentiation

T cells were purified from spleen with a T cell isolation kit (Miltenyi Biotec, Bergisch Gladbach, Germany). Cells (0.4×10^6) were placed on plate-bound anti-CD3 (2 μg/ml) and anti-CD28 (2.5 μg/ml) in 1 ml final volume RPMI 1640/5% FBS for 3 d. Th17 cells were obtained culturing anti-CD3/anti-CD28–activated T cells with IL-6 (50 ng/ml), TGF-β (1 ng/ml), anti–IL-4 (10 μg/ml), anti–IFN-γ (10 μg/ml), and FICZ (300 nM) for 3 d.

Cell lysis and Abs

IgE-sensitized BMMCs (5×10^6) were treated with 50 ng/ml Ag in RPMI 1640 medium for 8, 16, and 24 h, washed, and lysed. For some conditions, 300 nM FICZ was added to culture medium in the presence or absence of Ag. To inhibit AhR degradation, 7.5 μM MG-132 proteasome inhibitor was added to BMMCs together with FICZ for 4 h. BMMC lysates were prepared as in Sibilano et al. (15). Murine AhR, human AhR, and actin-detecting Ab were purchased from Enzo Life Sciences, Abcam (Cambridge, MA), and Sigma-Aldrich, respectively. Samples from 5×10^6 HepG2, LAD2, and HMC-1 cells were prepared as above. Percentage of protein expression was obtained from densitometric analysis of band intensity of AhR protein normalized to total actin.

Quantification of intracellular reactive oxygen species

Intracellular reactive oxygen species (ROS) were detected by incubating 2×10^5 BMMCs with 5 μM 5-(and-6)-chloromethyl-2′,7′-dichlorodihydrofluorescein diacetate acetyl ester (CM-H_2DCFDA; Sigma-Aldrich) 15 min before addition of 300 nM FICZ or 5 mM H_2O_2 as a positive control (Sigma-Aldrich). Thirty minutes later, cells were washed and relative fluorescence intensities were quantified by flow cytometric analysis (FL-1 channel). In some experiments, before CM-H_2DCFDA staining, BMMCs were either treated for 30 min with 1 mM Rp-cAMP or 10 mM NAC or with 300 nM FICZ for 16 and 3 h (repetitive treatment).

β-Hexosaminidase assay and cAMP quantification

IgE-presensitized BMMCs (5×10^5) in 250 μl Tyrode's buffer were challenged with 50 ng/ml Ag for 2.5, 5, 7.5, 10, and 30 min and the extent of degranulation was measured by percentage of β-hexosaminidase released. In some experiments, 300 nM FICZ was added at the same time as Ag. For repetitive treatment, FICZ was added to IgE-sensitized BMMCs for 16 h, and then cells were washed and fresh FICZ was added to cell culture for another 3 h before Ag. For cAMP quantification, 2×10^6 IgE-presensitized BMMCs were treated as above for 2, 5, 10, and 30 min and lysed in 200 μl 0.1 M HCl/0.1% Triton X-100. cAMP levels were measured with a Correlate-EIA direct cAMP enzyme immunoassay (Assay Designs, Enzo Live Sciences).

Systemic anaphylaxis

C57BL/6 mice were sensitized with 3 μg mouse Ag-specific IgE by i.v. injection 24 h before Ag challenge. For single dose treatment with FICZ, mice received 100 μg/kg body weight FICZ in 200 μl PBS in the presence or absence of 0.3 mg Ag. For repetitive treatment, mice were injected with 100 μg/kg body weight/200 μl FICZ 16 and 3 h before Ag. Then, 2.5 min upon Ag challenge, mice were euthanized and blood was collected by cardiac puncture for histamine ELISA quantification (Immunotech, Praha, Czech Republic).

Cytokine quantification

IgE-sensitized BMMCs (2×10^6/ml) or human MC lines HMC-1 and LAD2 were used for each condition. After 24 or 72 h with 300 nM FICZ, 50 ng/ml Ag, or Ag/FICZ stimulation, supernatants were collected and tested for IL-6 or IL-17 production (murine IL-6 and IL-17 ELISA from eBioscience, San Diego, CA; human IL-6 from Thermo Scientific, Waltham, MA; human IL-17 from Ray Biotech, Norcross, GA). For IL-17 production, where indicated, a 4-h extra stimulus consisting of 50 ng/ml PMA and 500 ng/ml ionomycin (both from Sigma-Aldrich) was given to BMMCs prior supernatant collection. IL-2 and INF-γ (CBA assay; Becton Dickinson, San Jose, CA), IL-5 and IL-13 (ELISA; PeproTech), and IL-4, IL-10, and IL-22 (ELISA; eBioscience) were measured in the supernatants of 72 h-stimulated cells. Supernatants for TNF-α were tested 12 h after stimulation (ELISA; eBioscience).

Selection of human samples

For in situ analyses, bioptic specimens of lung parenchyma from patients with severe COPD ($n = 4$) and control specimens ($n = 4$ samples of normal lung parenchyma) were collected from the archives of the Human Pa-

Downloaded from http://jimmunol.org/ at Inst Superiore de Sanita-Roma on June 4, 2012

thology Section, Department of Health Science, University of Palermo, Italy. All the procedures followed were in accordance with the Helsinki Declaration.

Histopathology and immunofluorescence

Histopathological analysis was performed on H&E and toluidine blue-stained sections cut from formalin-fixed, paraffin-embedded specimens. For in situ single-marker immunohistochemical analysis on lung tissue, sections were treated using a microwave epitope retrieval technique with 10 mmol citrate buffer (pH 9.0) at high temperature for 20 min and were incubated with anti-human tryptase and anti-human CD68 Abs (both from Novocastra, Newcastle, U.K.) overnight at 4°C. Staining was performed with UltraVision Quanto detection system HRP polymer (Thermo Scientific) and with 3,3′-diaminobenzidine substrate-chromogen (Thermo Scientific).

For in situ double-marker immunofluorescence on lung tissue, sections underwent two sequential rounds of single-marker immunostaining as previously reported (16). Anti-AhR (Abcam), anti–IL-6 (R&D Systems, USA), anti–IL-17 (R&D Systems, Minneapolis, MN), anti-CD2 (Novocastra), and anti-tryptase (Santa Cruz Biotechnology, Santa Cruz, CA) were adopted. After Fc blocking, Alexa Fluor-conjugated secondary Abs (Invitrogen) were used. Slides were evaluated using a Leica DMI6000 microscope, and microphotographs were collected using a Leica DFC350FX digital camera. Quantitative analysis of stained sections was performed by counting the absolute number of fluorescent cells out of four high-power microscopic fields (×400). Cells were counted by two expert pathologists (M.C., C.T.) in a blinded fashion.

Statistical analysis

Results are expressed as means ± SEM. Data were analyzed with a nonpaired Student *t* test (Prism; GraphPad Software, USA). Statistical significance is indicated as follows: $*p < 0.05$, $**p < 0.01$, $***p < 0.001$.

Results

BMMC degranulation is enhanced by transient AhR triggering and inhibited by prolonged AhR stimulation

Quantitative PCR analysis showed that AhR was expressed in BMMCs with levels comparable to Th17 cells (Fig. 1A). The presence of AhR in BMMCs was confirmed by Western blot analysis, which highlighted an ~90 kDa protein band in wild-type (WT), but not in AhR-deficient ($AhR^{-/-}$), BMMC lysate (Fig. 1B). AhR triggering was performed using FICZ, a small synthetic tryptophan-derivative compound, known to be a potent AhR agonist (17). FICZ at 300 nM, which was the highest concentration without effects on MC viability, was used throughout the in vitro experiments (Supplemental Fig. 1A). Twenty-four hours after FICZ exposure, AhR expression was reduced on the average of 64 ± 5% in the absence and 59 ± 5% in the presence of IgE-specific Ag, respectively compared with AhR levels found in unstimulated BMMCs (Fig. 1B). This finding is in accordance with previous works showing that the exposure to AhR agonists causes AhR-expressing cells to downregulate the receptor through the ubiquitin/proteasome degradation pathway (18, 19). To confirm that this pathway mediates AhR downregulation also in MCs, cells were treated with the proteasome inhibitor MG-132, together with FICZ for 4 h. This treatment blocked ligand-dependent degradation of AhR (Fig. 1C).

To study the role of AhR activation on MC responses to IgE triggering, BMMCs were incubated with or without FICZ, in the presence or absence of Ag. Degranulation was measured through the release of MC granule-associated enzyme β-hexosaminidase at different time points (Fig. 2A). FICZ treatment did not influence degranulation in the absence of antigenic stimulation, whereas it enhanced granule exocytosis at early stages of Ag response, for example, 2.5, 5, and 7.5 min following Ag triggering (2.5 min: Ag, 20.25 ± 1.57%, Ag/FICZ, 31.12 ± 4.07%; 5 min: Ag, 25.42 ± 0.27%, Ag/FICZ, 31.11 ± 0.74%; 7.5 min, Ag: 31.95 ± 0.19%, Ag/FICZ, 35.25 ± 0.50% β-hexosaminidase release; $p = 0.03$, 0.0004, and 0.002, respectively). This effect was AhR-specific, since AhR-deficient BMMCs, whose FcεRI expression levels were similar to WT BMMCs (Supplemental Fig. 1B), did not display upregulation of β-hexosaminidase release upon FICZ treatment (Fig. 2B). The consequence of in vivo AhR stimulation on MC degranulation was then investigated in a model of passive systemic anaphylaxis, known to be dependent on MC activity. FICZ and Ag concurrent administration in mice caused a significant and prompt increase in plasma histamine levels (measured 2.5 min after challenge), compared with Ag administration alone (Fig. 2C; Ag, 931.7 ± 82.4 ng/ml histamine; Ag/FICZ, 1389 ± 128.2 ng/ml histamine; $p = 0.008$).

Because the presence of AhR ligands in the environment may determine a repeated stimulation of AhR, the downstream responses might differ from that activated by a single AhR triggering. To address this issue, BMMCs were treated twice with different schedules of 300 nM FICZ (Supplemental Fig. 1C). In all conditions tested, degranulation was reduced, with the greatest effect reached when FICZ was administered 16 and 3 h before Ag triggering, in which degranulation was reduced in WT BMMCs (Fig. 2D; Ag alone, 41.5 ± 0.4% β-hexosaminidase; pre-exposure to FICZ/Ag, 18.5 ± 2.8% β-hexosaminidase; $p = 0.015$), but not in AhR-deficient BMMCs (Fig. 2E). In this study, AhR protein expression was decreased, but still detectable (Fig. 2F). Similarly, in in vivo experiments of systemic anaphylaxis, repeated treatment with FICZ caused a reduced release of histamine upon Ag challenge, as compared with Ag challenge alone (Fig. 2G; Ag, 3376 ± 512.2 ng/ml histamine; pre-exposure to FICZ/Ag, 1490 ± 180.5 ng/ml histamine; $p = 0.008$).

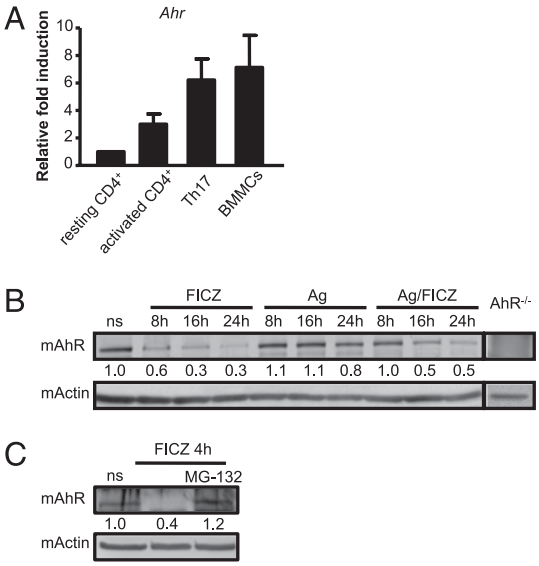

FIGURE 1. BMMCs express AhR, which is degraded via proteasome upon FICZ ligation. (**A**) Quantitative PCR to compare levels of AhR mRNA among resting or anti-CD3/anti-CD28–activated $CD4^+$ T cells, differentiated Th17 cells, and BMMCs. Results are expressed as fold induction over resting $CD4^+$ T cells. Means ± SEM from three independent experiments are shown. (**B**) Western blot analysis to verify AhR presence in lysates from WT BMMCs, normalized to total actin. IgE-sensitized BMMCs were left unstimulated (ns) or stimulated with FICZ, Ag, or Ag/FICZ at indicated time points. Unstimulated AhR-deficient ($AhR^{-/-}$) BMMCs were used as control. Numbers indicate protein fold expression relative to unstimulated BMMCs. (**C**) IgE-sensitized BMMCs were treated with FICZ without or with 7.5 μM proteasome inhibitor MG-132 for 4 h. Lysates were normalized to total actin and numbers indicate protein fold expression relative to unstimulated BMMCs. One of three experiments is shown.

Downloaded from http://jimmunol.org/ at Inst Superiore de Sanita-Roma on June 4, 2012

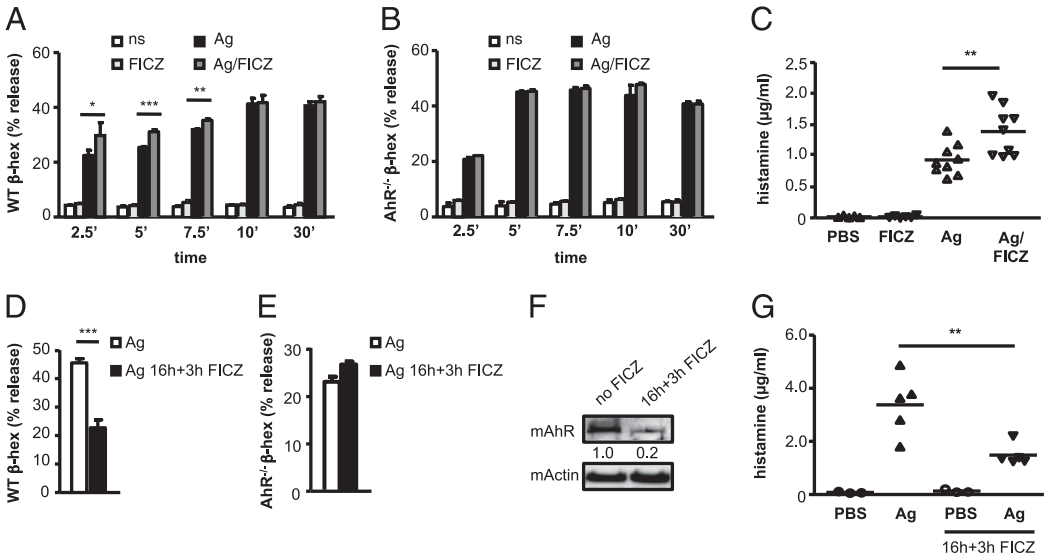

FIGURE 2. BMMC responsiveness to FICZ depends on treatment schedule. (**A** and **B**) Time course BMMC degranulation assay. (A) IgE-sensitized WT BMMCs were stimulated with FICZ in the absence or presence of Ag and examined for β-hexosaminidase (β-hex) release at indicated time points. (B) IgE-sensitized AhR-deficient ($AhR^{-/-}$) BMMCs were stimulated and examined for β-hexosaminidase release as in (A). Numbers indicate means ± SEM from three independent experiments. (**C**) In vivo plasma histamine levels were measured 2.5 min upon challenge with PBS ($n = 5$), FICZ ($n = 5$), Ag ($n = 9$), and Ag/FICZ ($n = 9$). (**D** and **E**) IgE-sensitized WT or $AhR^{-/-}$ BMMCs were untreated or treated with FICZ for 16 and 3 h (16h+3h FICZ) before Ag addition. β-hexosaminidase was quantified 30 min after Ag addition. Numbers indicate means ± SEM from two independent experiments. (**F**) AhR protein expression after 16h+3h FICZ treatment. Lysates were normalized to total actin, and numbers indicate protein fold expression relative to unstimulated BMMCs. One of three experiments is shown. (**G**) In vivo plasma histamine levels were measured as in (C). Mice were untreated or treated 16 and 3 h with FICZ (16h+3h FICZ) and challenged with PBS ($n = 3$) or with Ag ($n = 5$). $*p < 0.05$, $**p < 0.01$, $***p < 0.001$.

FICZ modulates cAMP, which is necessary for FcεRI-dependent degranulation and ROS production in BMMCs

A shared intracellular mechanism regulating AhR-related functions and FcεRI-dependent MC degranulation involves the cAMP signaling, which is necessary for AhR translocation to the nucleus and activation of reporter genes in many cell types (20), as well as for appropriate MC granule exocytosis following FcεRI activation (21). Thus, the effect of AhR triggering, either alone or in combination with FcεRI crosslinking, on cAMP production was evaluated. Single exposure to FICZ, concomitantly with Ag challenge, significantly enhanced intracellular cAMP production at 2 and 5 min, compared with untreated BMMCs, in WT (Fig. 3A; 2 min, 4.3 ± 0.2-fold, $p = 0.016$; 5 min, 2.8 ± 0.1-fold, $p = 0.014$), but not in AhR-deficient BMMCs (Fig. 3B). Interestingly, in the absence of Ag, single exposure to FICZ was able to transiently and rapidly enhance cAMP levels in WT BMMCs (Fig. 3C). On the contrary, 16 and 3 h FICZ pretreatment reduced intracellular cAMP levels in response to the Ag in WT BMMCs but not in AhR-deficient BMMCs (Fig. 3D), suggesting that repetitive exposure to FICZ renders BMMCs anergic in cAMP production.

Because of the AhR-dependent proinflammatory scenario (5) and the ability of MCs to produce ROS during inflammatory and allergic responses (22), we analyzed whether AhR ligands lead to ROS production. WT BMMCs, stained with the fluorescent dye CM-H_2DCFDA, consistently produced ROS in response to a single dose of FICZ (Fig. 3E). This was not observed in AhR-deficient BMMCs (Fig. 3F). To study the role of cAMP/PKA signals on AhR-induced ROS production, BMMCs were pretreated with the PKA inhibitor Rp-cAMP. With these settings, AhR-mediated ROS formation was inhibited (Fig. 3G). As for cAMP (Fig. 3D), upon 16 and 3 h stimulation with FICZ, ROS production was impaired (Fig. 3H), confirming that repetitive AhR activation confers anergy to MCs.

FICZ stimulation sets the stage for the proinflammatory milieu by inducing IL-6 and IL-17 production in murine and human MCs

AhR is widely considered a key factor in driving the fate of Th17 differentiation (5) and in inducing IL-6 production itself (23), whereas MCs represent a potent source of IL-6 and IL-17 in many pathological conditions such as in the synovium in rheumatoid arthritis, in osteoarthritis, and in psoriatic lesions (24–26). On these bases, we investigated whether direct exposure to FICZ could drive MCs to release IL-6 and IL-17. FICZ treatment induced BMMC IL-6 production that was slightly increased by concomitant Ag stimulation (Fig. 4A, open bars; FICZ, 155.9 ± 15.6 pg/ml; Ag, 1204.7 ± 53.2 pg/ml; Ag/FICZ, 1417.9 ± 14.1 pg/ml), an effect absent in AhR-deficient BMMCs (Fig. 4A, filled bars). AhR induces IL-6 production, in a human monocytic cell line, via cAMP-dependent PKA activation (27). To test whether AhR-induced cAMP correlates with IL-6 secretion, we used the PKA inhibitor Rp-cAMP. Results showed that FICZ-induced IL-6 production was lowered in both unstimulated and Ag-stimulated BMMCs in which the cAMP/PKA pathway was transiently inhibited by Rp-cAMP (Fig. 4B; FICZ, 67.4 ± 0.4 pg/ml; Rp-cAMP/FICZ, 34.1 ± 10.2 pg/ml; Ag/FICZ, 1070 ± 9.2 pg/ml; Ag/Rp-cAMP/FICZ, 761.7 ± 10.8 pg/ml).

BMMC-derived IL-17 was evaluated as detailed for IL-6. After 72 h exposure to a single-dose of FICZ, BMMCs produced low levels of IL-17 (Fig. 4C; FICZ, 70.1 ± 0.4 pg/ml; Ag/FICZ, 86.0 ± 6.4 pg/ml). To confirm FICZ-induced IL-17 production by BMMCs, we provided an extra 4 h stimulus with PMA/ionomycin known to enhance gene transcription. With this treatment, we were able to detect a high basal level for IL-17 production, which appeared further increased in the presence of Ag stimulation and was enhanced by FICZ (Fig. 4D). Upon FICZ exposure, IL-17–producing BMMCs were also detected through FACS analysis (Supplemental Fig. 2A).

Downloaded from http://jimmunol.org/ at Inst Superiore de Sanita-Roma on June 4, 2012

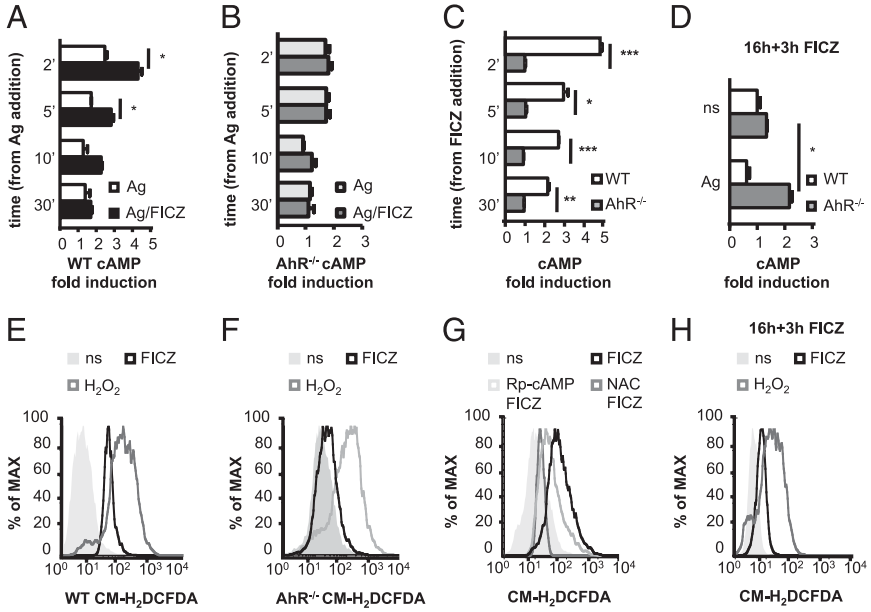

FIGURE 3. FICZ regulates cAMP and ROS levels in BMMCs. (**A**) IgE-sensitized WT BMMCs were stimulated with Ag in the absence (Ag, open bars) or presence of FICZ (Ag/FICZ, filled bars), and at the indicated time points cAMP intracellular levels were measured. (**B**) IgE-sensitized AhR$^{-/-}$ BMMCs were stimulated as in (A), and cAMP levels were measured. (**C**) In the absence of Ag stimulation, WT (white bars) or AhR-deficient (AhR$^{-/-}$, gray bars) BMMCs were treated with FICZ as in (A). (**D**) WT (white bars) and AhR-deficient BMMCs (AhR$^{-/-}$, gray bars) were treated for 16 and 3 h with FICZ, IgE-sensitized, and triggered with Ag for 5 min. (A–D) Numbers indicate cAMP fold induction over unstimulated BMMCs and are the means ± SEM from at least two independent experiments for each panel. (**E**) WT BMMCs were untreated (ns, gray histogram) or treated with FICZ (black line) or H_2O_2 (gray line) and stained with ROS-specific dye CM-H_2DCFDA. (**F**) AhR$^{-/-}$ BMMCs were treated and stained as in (E). (**G**) BMMCs were pretreated with PKA antagonist Rp-cAMP (Rp-cAMP+FICZ, light gray line) or with NAC, used as control to lower ROS production (NAC+FICZ, dark gray line), stained, and analyzed as in (E). (**H**) WT BMMCs were pretreated for 16 and 3 h with FICZ, stained, and analyzed as in (E). Results from one representative experiment of three are shown. $*p < 0.05$, $**p < 0.01$, $***p < 0.001$.

The analysis of cytokine production was extended to Th1/Th2, regulatory cytokines, and IL-22, which is coexpressed with IL-17 by Th17 cells (28). We found that, besides IL-17 and IL-6, FICZ induced BMMC production of the proinflammatory IL-13 and the regulatory IL-10 cytokines. Interestingly, the detection of the early released mediator TNF-α, a classical cytokine that MCs can release upon Ag stimulation, was slightly enhanced in the copresence of Ag and FICZ (Table I).

We subsequently investigated AhR expression and function in human MCs. As shown in Fig. 4E, human MC lines HMC-1 and LAD2 expressed AhR at different levels. Similar to murine BMMCs, AhR stimulation by FICZ alone led to IL-6 (Fig. 4F, filled bar; HMC-1, 68.9 ± 29.7 pg/ml; LAD2, 79.1 ± 4.5 pg/ml) and IL-17 production (Fig. 4G, filled bar; HMC-1, not detected; LAD2, 306.0 ± 17.50 pg/ml). The latter was increased upon an extra PMA/ionomycin stimulation (Fig. 4H, filled bar; HMC-1, 112.3 ± 41.1 pg/ml; LAD2, 459.8 ± 32.8 pg/ml).

Mast cells from COPD patients express AhR and are a relevant in situ source of IL-6 and IL-17

The presence of AhR$^+$ MCs, as well as the number of AhR$^+$ cells expressing IL-6 and IL-17, was assessed in lung specimens of COPD patients by double immunofluorescence in situ. Overall, a significantly increased number of MCs infiltrating the epithelial layer and the lamina propria of the bronchial mucosa was detected in samples from COPD patients as compared with controls (Fig. 5A, 5C, toluidine blue and tryptase). Besides MCs, other innate immune cells proved to be increased in the lung parenchyma of patients with severe COPD (dendritic cell-SIGN-positive myeloid dendritic cells and myeloperoxidase-positive granulocytes; data not shown). However, differently from MCs, macrophages mainly localized within the lamina propria of the bronchus mucosa and in the interstitium between the alveoli, only rarely extending inside the epithelium (Fig. 5A, 5C, CD68, toluidine blue, and tryptase). These data suggest MCs as the innate immune cells chiefly involved as sensors of epithelial damage in the bronchus mucosa.

In COPD and control samples, AhR was comparably expressed by epithelial cells (Fig. 5B, 5D), while characterizing a higher number of tryptase-expressing MCs in COPD samples, compared with controls. Moreover, COPD samples displayed a high amount of AhR$^+$/IL-6$^+$ and AhR$^+$/IL-17$^+$ nonepithelial cells in the lamina propria, which supported the contribution of AhR-expressing cells in the molding of COPD inflammatory microenvironment. The difference in the amount of AhR$^+$/IL-6$^+$ and AhR$^+$/IL-17$^+$ cells observed between COPD and control samples was paralleled by that of the amount of tryptase$^+$/IL-6$^+$ and tryptase$^+$/IL-17$^+$ MCs, implicating MCs as the relevant source of IL-6 and IL-17 (Fig. 5D, 5E). Other tryptase-negative IL-17–producing cells were also detected within the bronchial mucosal interface, which mainly proved to be of T cell phenotype, as they expressed the CD2 marker (e.g., Th17 cells and/or TCRγδ T cells).

Discussion

AhR functional expression has been reported in NK T cells, TCRγδ T cells, macrophages, and dendritic cells, all located at the interface between innate and acquired immune system (25, 29, 30), suggesting that environmental factors as well as metabolic products have a role in the development of local cells and immune response. In this study, to our knowledge we show for the first time that murine and human MCs constitutively express AhR, whose activation by FICZ is able to influence both FcεRI-mediated early degranulation response and FcεRI-independent IL-6 and IL-17 cytokine production.

Downloaded from http://jimmunol.org/ at Inst Superiore de Sanita-Roma on June 4, 2012

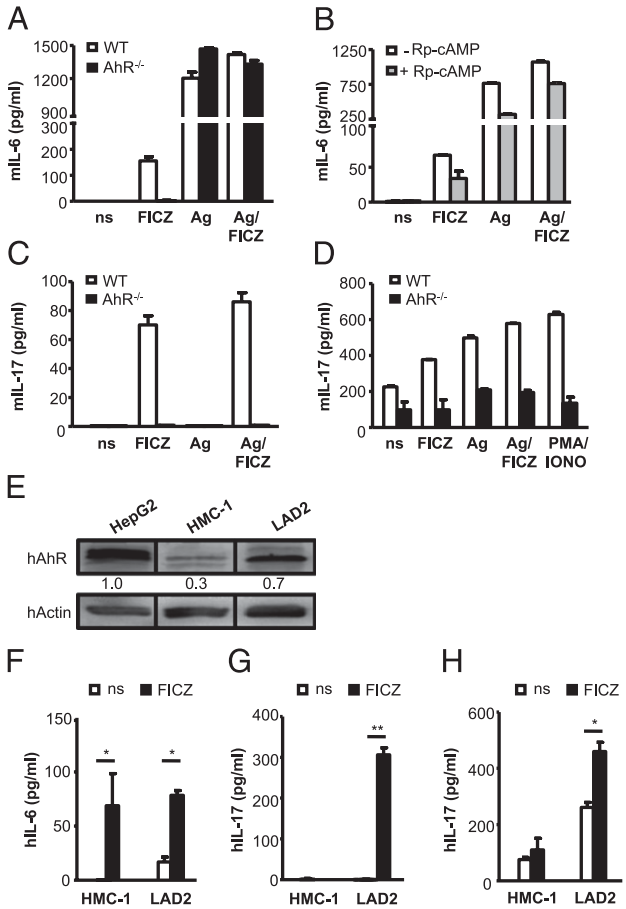

FIGURE 4. Murine and human MCs respond to FICZ by producing IL-6 and IL-17. (**A**) IL-6 presence was evaluated by ELISA in the supernatants of WT (open bars) and AhR-deficient IgE-sensitized BMMCs ($AhR^{-/-}$, filled bars) untriggered (ns) or triggered with Ag in the absence or presence FICZ for 24 h. (**B**) IL-6 presence was evaluated as in (A) in BMMCs not treated (− Rp-cAMP, open bars) or pretreated with PKA antagonist Rp-cAMP (+ Rp-cAMP, filled bars). (**C**) IL-17 presence was measured in the same conditions shown in (A), but supernatants were collected 72 h after addition of stimuli. (**D**) IL-17 was measured as in (C) with an extra 4 h stimulus with 50 ng/ml PMA and 500 ng/ml ionomycin (IONO) prior to collection of supernatants. As positive control condition, BMMCs were treated 72 h with 10 ng/ml PMA and 100 ng/ml ionomycin. For (A)–(D), numbers indicate means ± SEM of one representative of at least three independent experiments. (**E**) Western blot analysis for AhR presence in lysates from HepG2 human liver carcinoma cell line (positive control for AhR) as well as human MC lines HMC-1 and LAD2 normalized to total actin. Numbers indicate fold expression relatively to HepG2 cell line. (**F** and **G**) IL-6 or IL-17 was evaluated by ELISA in the supernatants of LAD2 and HMC-1 cells, after 24 or 72 h stimulation with FICZ, respectively. (**H**) IL-17 was measured as in (G) with an extra 4 h stimulus with 50 ng/ml PMA and 500 ng/ml ionomycin (IONO) prior to collection of supernatants. For panels (F)–(H), numbers indicate means ± SEM from at least two independent experiments. $*p < 0.05$, $**p < 0.01$.

BMMCs showed opposite responses to the Ag-dependent activation, according to the timing of exposure to FICZ. Single-dose administration of FICZ together with the Ag enhanced IgE/Ag-dependent MC activation, whereas repeated treatment rendered MCs less responsive to antigenic stimulation both in vivo and in vitro. In this regard, we might speculate that MC hyperresponsiveness may be associated with abrupt and intense exposure to AhR ligands commonly spread in industrialized countries (e.g., dioxins, airborne pollutants, tryptophan-rich dietary compounds), which may correlate with the onset of allergy and allergy-related pathologies in young individuals who encounter these compounds together with the allergen for the first time (31). Strikingly, FICZ-dependent formation of ROS observed in our experiments would also be in accordance and contribute to the enhancement of the overall inflammatory acute response observed in young allergic patients (32). Alternatively, repetitive exposure to AhR-ligand pollutants could suppress MC degranulation and attenuate the allergic response in favor of other types MC-mediated responses (e.g., inflammatory responses) by directly acting on AhR-mediated MC responsiveness (10). Consistently, MC "desensitization" through a repetitive AhR activation may suggest an association with approaching therapies to desensitize patients (especially children) that develop severe IgE-mediated anaphylactic responses against dietary compounds (33).

However, it remains to be fully established how repetitive exposure to AhR agonists reduced IgE-induced MC degranulation since levels of FcεRI molecules present on MC surface remained unaffected during treatment with FICZ (data not shown). We identified cytosolic cAMP, whose rapid and transient increase is required for MC exocytosis of granule content following FcεRI triggering (21), as a crucial mediator responsible for many effects caused by agonist-activated AhR in MCs. Indeed, upon single dose exposure to FICZ, we observed a transient boost in cAMP production that enhanced Ag-dependent degranulation, whereas after double exposure to FICZ, BMMCs were no longer able to upregulate cAMP. This could be due to either direct adenylate cyclase inhibition or enhancement of phosphodiesterase amount and/or activity, which prevents AhR function.

Interestingly, the increase of cAMP content in the absence of antigenic stimulation was not per se sufficient to induce degranulation in MCs, but it was adequate for ROS generation. The role of cAMP/PKA signals on ROS production is still debated, and opposite effects have been reported, depending on the compound used to generate ROS and the cellular model used (34, 35). Our data showed that FICZ-dependent increase of cAMP leads to ROS production, as pretreatment with the transient PKA inhibitor Rp-cAMP prevented FICZ-induced ROS formation both in murine and human (data not shown) MCs.

The cAMP/PKA pathway induces IL-6 production in different cell types (36, 37), and AhR activation is able to induce IL-6 production by de-repressing its promoter in tumor cell lines (23). Accordingly, our findings revealed a close relationship between AhR stimulation, cAMP, and cAMP-dependent IL-6 production. Indeed, the use of the transient PKA inhibitor Rp-cAMP partially inhibited IL-6 production from FICZ-, Ag-, and Ag/FICZ-stimulated BMMCs.

We have recently demonstrated the importance of MC-produced IL-6 in mediating the inhibition of Treg cell suppression toward Th17 differentiation (9) and, in this study, we show that a single compound is able to skew MCs toward IL-6, IL-17, and IL-13 production by specifically activating AhR. The consequences of this event could be now evaluated in diseases where MCs represent a potent source of proinflammatory cytokines and exposure to AhR ligands is likely to occur (38). For instance, MCs alone or together with other non-T immune cells are predominant IL-17^{+} cells in psoriatic lesions in human skin (25), in atherosclerotic plaques (39), as well as in rheumatoid arthritis, osteoarthritis, and spondyloarthritis synovium (24, 26, 40). Human MCs require the Th17 lineage-defining transcription factor *Rorc* to produce IL-17 in response to different stimuli (24). In this study, we were not able to detect *Rorc* in both unstimulated and FICZ-stimulated BMMCs (Supplemental Fig. 2B). This result opens the perspective that, at least for murine BMMCs, MCs are also eligible to use a proper pathway to induce IL-17 transcription after FICZ exposure.

Downloaded from http://jimmunol.org/ at Inst Superiore de Sanita-Roma on June 4, 2012

Table I. Cytokine production of murine BMMCs in response to FICZ

	ns	FICZ	Ag	Ag/FICZ
IL-2, IL-4, IL-5, IL-22, IFN-γ	n.d.	n.d.	n.d.	n.d.
IL-10	n.d.	170.0 ± 45.0***	n.d.	150.0 ± 25.0***
IL-13	n.d.	99.7 ± 21.7***	183.0 ± 1.7	179.7 ± 18.3
TNF-α	53.3 ± 1.6	46.7 ± 5.0	406.7 ± 5.0	496.7 ± 18.3*

IL-2, IL-4, IL-10, INF-γ, IL-5, IL-13, and IL-22 were evaluated in the supernatants of IgE-sensitized BMMCs untriggered (ns) or triggered with 50 ng/ml Ag (IgE/Ag) in the absence or presence of 300 nM FICZ for 72 h. Supernatants for TNF-α were tested by ELISA 12 h after stimulation. Results are expressed as means ± SEM from at least two independent experiments.
*$p < 0.05$, ***$p < 0.001$, compared with FICZ-untreated BMMCs.
n.d., Not detectable.

The main cause ascribed to the pathogenesis of COPD is the exposure to cigarette smoke, which induces chronic inflammation of the bronchial mucosa. Cigarette smoke contains several polycyclic aromatic hydrocarbons and dioxins, known to function as AhR ligands. IL-6 and IL-17 have been extensively detected in the lungs of COPD patients (11). Although various therapeutical approaches based on neutralizing Ab against proinflammatory cytokines have been proposed to attenuate airway inflammation in COPD (41, 42), the main source and the precise role of IL-6 and IL-17 in this disease remain undefined. Conflicting results have been also reported for the role of AhR in immunological responses in the airways. Chiba et al. (43) have reported that AhR activation in airway epithelial cells induces mucin secretion through production of ROS, suggesting that antioxidant treatments may be appropriate for patients with respiratory symptoms related to dioxin exposure. On the contrary, Baglole et al. (44) have shown that AhR activation by cigarette smoke extracts has a protective effect on airway inflammation by inducing the production of the cytoprotective enzyme heme-oxygenase-1 by lung fibroblasts. The discrepancy between these results may be ascribed to the model (human versus mouse cell lines), the mechanism (structural damage versus inflammation), and AhR agonists adopted. In this study, we show that AhR-positive MCs appear to be one of the major sources of IL-6 and IL-17 in bronchial biopsies from COPD patients. AhR positivity observed in human MCs could be ascribed to the loss of mechanisms controlling AhR expression, due to the potential prolonged exposure to AhR ligands in COPD patients. These changes may represent, for example, the loss of the AhR repressor and/or of proteasome functionality in damaged tissues. Nevertheless, whether MCs are central to or supportive for the pathogenesis of airway diseases remains to be clarified. Airway MCs, exposed to environmental Ags, may be activated via AhR and secrete proinflammatory mediators, generating a process that culminates in chronic inflammation. In particular, MC-derived IL-17 may contribute to the progress of inflammation, inducing epithelial cells to promote neutrophil accumulation into the site of injury. Moreover, IL-6 and IL-13 production are also associated with a pattern of airway remodeling (45), contributing to the overall worsening of the disease.

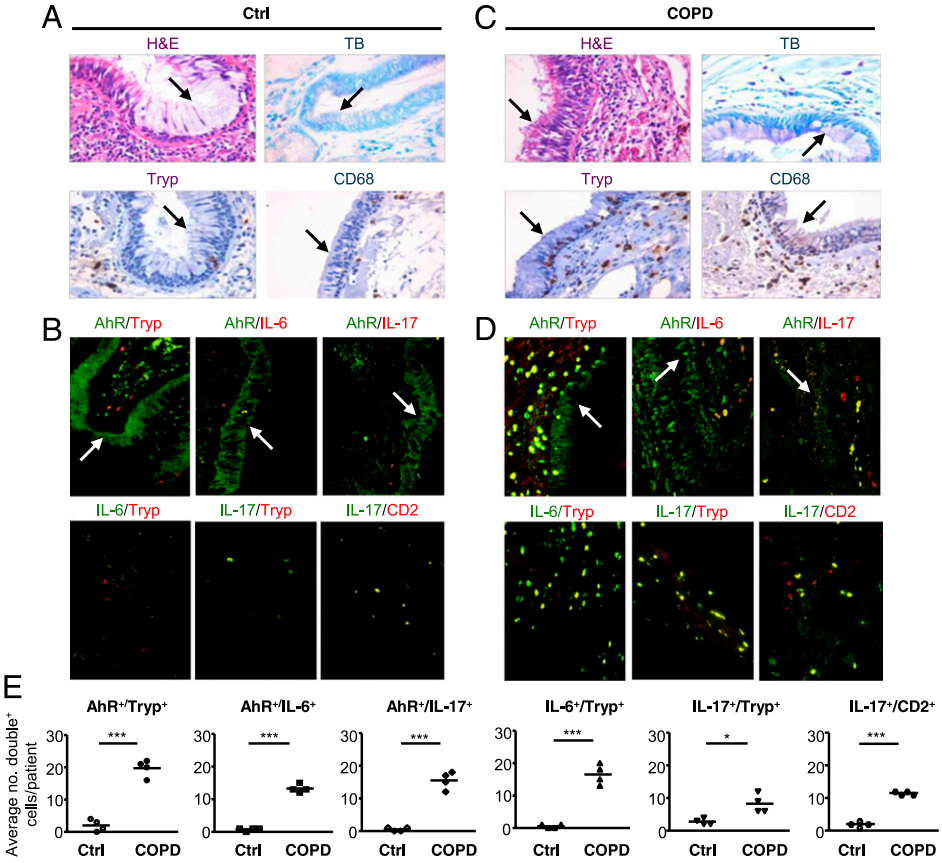

FIGURE 5. Presence of tryptase-, AhR-, IL-6–, and IL-17–positive cells in bronchial biopsies from COPD patients. (**A**) H&E, toluidine blue (TB), tryptase (Tryp), and CD68 staining of sections from normal lung parenchyma (Ctrl). (**B**) Double-marker immunofluorescence analysis of AhR-, tryptase (Tryp)-, IL-6–, IL-17–, and CD2-positive cells in sections from normal lung parenchyma (double stainings: AhR/Tryp: AhR green, Tryp red; IL-6/Tryp, IL-6 green, Tryp red; AhR/IL-6, AhR green, IL-6 red; IL-17/Tryp, IL-17 green, Tryp red; AhR/IL-17, AhR green, IL-17 red; IL-17/CD2: IL-17 green, CD2 red. Original magnification, ×40). (**C** and **D**) Samples from COPD patients were stained as in (A) and (B), respectively. Arrows indicate epithelial cells. (**E**) Counts of AhR/Tryp ($AhR^+/Tryp^+$), IL-6/Tryp ($IL\text{-}6^+/Tryp^+$), AhR/IL-6 ($AhR^+/IL\text{-}6^+$), IL-17/Tryp ($IL\text{-}17^+/Tryp^+$), and AhR/IL-17 ($AhR^+/IL\text{-}17^+$) double-positive cells in bronchial mucosa from four controls (Ctrl) and four COPD samples. Cells were detected and counted out of four ×400 high-power microscopic fields in each case. Each symbol in graphs represents the average of double-positive cells for each case, obtained as indicated. *$p < 0.05$, ***$p < 0.001$.

Downloaded from http://jimmunol.org/ at Inst Superiore de Sanita-Roma on June 4, 2012

Our study highlights a new and previously unappreciated role of MCs through AhR activation in orchestrating inflammatory responses. This could be extended to all those pathologies where tissue/organ homeostasis is broken by an inflammatory MC-rich infiltrate, likely accessible by AhR ligands derived from tryptophan metabolism, such as inflammatory bowel disease (3) and eosinophilia-myalgia syndrome (46).

Our results lay the bases for forthcoming studies aimed at a deeper understanding of the role of AhR in modulating MC effector functions.

Acknowledgments

We thank Drs. Juan Rivera, Ryo Suzuki, and Charlotte Esser for material support, as well as Dr. Silvia Piconese for helpful discussion.

Disclosures

The authors have no financial conflicts of interest.

References

1. Gu, Y. Z., J. B. Hogenesch, and C. A. Bradfield. 2000. The PAS superfamily: sensors of environmental and developmental signals. *Annu. Rev. Pharmacol. Toxicol.* 40: 519–561.
2. Marshall, N. B., and N. I. Kerkvliet. 2010. Dioxin and immune regulation: emerging role of aryl hydrocarbon receptor in the generation of regulatory T cells. *Ann. N. Y. Acad. Sci.* 1183: 25–37.
3. Monteleone, I., A. Rizzo, M. Sarra, G. Sica, P. Sileri, L. Biancone, T. T. Macdonald, F. Pallone, and G. Monteleone. 2011. Aryl hydrocarbon receptor-induced signals up-regulate IL-22 production and inhibit inflammation in the gastrointestinal gract. *Gastroenterology* 141: 237–248.
4. Baglole, C. J., S. B. Maggirwar, T. A. Gasiewicz, T. H. Thatcher, R. P. Phipps, and P. J. Sime. 2008. The aryl hydrocarbon receptor attenuates tobacco smoke-induced cyclooxygenase-2 and prostaglandin production in lung fibroblasts through regulation of the NF-κB family member RelB. *J. Biol. Chem.* 283: 28944–28957.
5. Esser, C., A. Rannug, and B. Stockinger. 2009. The aryl hydrocarbon receptor in immunity. *Trends Immunol.* 30: 447–454.
6. Gandhi, R., D. Kumar, E. J. Burns, M. Nadeau, B. Dake, A. Laroni, D. Kozoriz, H. L. Weiner, and F. J. Quintana. 2010. Activation of the aryl hydrocarbon receptor induces human type 1 regulatory T cell-like and Foxp3$^+$ regulatory T cells. *Nat. Immunol.* 11: 846–853.
7. Quintana, F. J., A. S. Basso, A. H. Iglesias, T. Korn, M. F. Farez, E. Bettelli, M. Caccamo, M. Oukka, and H. L. Weiner. 2008. Control of T_{reg} and T_H17 cell differentiation by the aryl hydrocarbon receptor. *Nature* 453: 65–71.
8. Tsai, M., M. Grimbaldeston, and S. J. Galli. 2011. Mast cells and immunoregulation/immunomodulation. *Adv. Exp. Med. Biol.* 716: 186–211.
9. Piconese, S., G. Gri, C. Tripodo, S. Musio, A. Gorzanelli, B. Frossi, R. Pedotti, C. E. Pucillo, and M. P. Colombo. 2009. Mast cells counteract regulatory T-cell suppression through interleukin-6 and OX40/OX40L axis toward Th17-cell differentiation. *Blood* 114: 2639–2648.
10. Schulz, V. J., J. J. Smit, K. J. Willemsen, D. Fiechter, I. Hassing, R. Bleumink, L. Boon, M. van den Berg, M. B. M. van Duursen, and R. H. H. Pieters. 2011. Activation of the aryl hydrocarbon receptor suppresses sensitization in a mouse peanut allergy model. *Toxicol. Sci.* 123: 491–500.
11. Brusselle, G. G., G. F. Joos, and K. R. Bracke. 2011. New insights into the immunology of chronic obstructive pulmonary disease. *Lancet* 378: 1015–1026.
12. Andersson, C. K., M. Mori, L. Bjermer, C.-G. Löfdahl, and J. S. Erjefält. 2010. Alterations in lung mast cell populations in patients with chronic obstructive pulmonary disease. *Am. J. Respir. Crit. Care Med.* 181: 206–217.
13. Liu, F. T., J. W. Bohn, E. L. Ferry, H. Yamamoto, C. A. Molinaro, L. A. Sherman, N. R. Klinman, and D. H. Katz. 1980. Monoclonal dinitrophenyl-specific murine IgE antibody: preparation, isolation, and characterization. *J. Immunol.* 124: 2728–2737.
14. Gri, G., S. Piconese, B. Frossi, V. Manfroi, S. Merluzzi, C. Tripodo, A. Viola, S. Odom, J. Rivera, M. P. Colombo, and C. E. Pucillo. 2008. CD4$^+$CD25$^+$ regulatory T cells suppress mast cell degranulation and allergic responses through OX40-OX40L interaction. *Immunity* 29: 771–781.
15. Sibilano, R., G. Gri, B. Frossi, C. Tripodo, R. Suzuki, J. Rivera, A. S. MacDonald, and C. E. Pucillo. 2011. Technical advance: soluble OX40 molecule mimics regulatory T cell modulatory activity on FcεRI-dependent mast cell degranulation. *J. Leukoc. Biol.* 90: 831–838.
16. Tripodo, C., G. Gri, P. P. Piccaluga, B. Frossi, C. Guarnotta, S. Piconese, G. Franco, V. Vetri, C. E. Pucillo, A. M. Florena, et al. 2010. Mast cells and Th17 cells contribute to the lymphoma-associated pro-inflammatory microenvironment of angioimmunoblastic T-cell lymphoma. *Am. J. Pathol.* 177: 792–802.
17. Wincent, E., N. Amini, S. Luecke, H. Glatt, J. Bergman, C. Crescenzi, A. Rannug, and U. Rannug. 2009. The suggested physiologic aryl hydrocarbon receptor activator and cytochrome P4501 substrate 6-formylindolo[3,2-*b*]carbazole is present in humans. *J. Biol. Chem.* 284: 2690–2696.
18. Davarinos, N. A., and R. S. Pollenz. 1999. Aryl hydrocarbon receptor imported into the nucleus following ligand binding is rapidly degraded via the cytosplasmic proteasome following nuclear export. *J. Biol. Chem.* 274: 28708–28715.
19. Harper, P. A., D. S. Riddick, and A. B. Okey. 2006. Regulating the regulator: factors that control levels and activity of the aryl hydrocarbon receptor. *Biochem. Pharmacol.* 72: 267–279.
20. Oesch-Bartlomowicz, B., A. Huelster, O. Wiss, P. Antoniou-Lipfert, C. Dietrich, M. Arand, C. Weiss, E. Bockamp, and F. Oesch. 2005. Aryl hydrocarbon receptor activation by cAMP vs. dioxin: divergent signaling pathways. *Proc. Natl. Acad. Sci. USA* 102: 9218–9223.
21. Austen, K. F. 1980. Chemical mediators originating from human mast cells: a commentary. *Clin. Allergy* 10(Suppl.): 477–479.
22. Swindle, E. J., and D. D. Metcalfe. 2007. The role of reactive oxygen species and nitric oxide in mast cell-dependent inflammatory processes. *Immunol. Rev.* 217: 186–205.
23. DiNatale, B. C., J. C. Schroeder, L. J. Francey, A. Kusnadi, and G. H. Perdew. 2010. Mechanistic insights into the events that lead to synergistic induction of interleukin 6 transcription upon activation of the aryl hydrocarbon receptor and inflammatory signaling. *J. Biol. Chem.* 285: 24388–24397.
24. Hueber, A. J., D. L. Asquith, A. M. Miller, J. Reilly, S. Kerr, J. Leipe, A. J. Melendez, and I. B. McInnes. 2010. Mast cells express IL-17A in rheumatoid arthritis synovium. *J. Immunol.* 184: 3336–3340.
25. Lin, A. M., C. J. Rubin, R. Khandpur, J. Y. Wang, M. Riblett, S. Yalavarthi, E. C. Villanueva, P. Shah, M. J. Kaplan, and A. T. Bruce. 2011. Mast cells and neutrophils release IL-17 through extracellular trap formation in psoriasis. *J. Immunol.* 187: 490–500.
26. Suurmond, J., A. L. Dorjée, M. R. Boon, E. F. Knol, T. W. Huizinga, R. E. Toes, and A. J. Schuerwegh. 2011. Mast cells are the main interleukin 17-positive cells in anticitrullinated protein antibody-positive and -negative rheumatoid arthritis and osteoarthritis synovium. *Arthritis Res. Ther.* 13: R150.
27. Vogel, C. F. A., E. Sciullo, W. Li, P. Wong, G. Lazennec, and F. Matsumura. 2007. RelB, a new partner of aryl hydrocarbon receptor-mediated transcription. *Mol. Endocrinol.* 21: 2941–2955.
28. McAleer, J. P., and J. K. Kolls. 2011. Mechanisms controlling Th17 cytokine expression and host defense. *J. Leukoc. Biol.* 90: 263–270.
29. Frericks, M., M. Meissner, and C. Esser. 2007. Microarray analysis of the AHR system: tissue-specific flexibility in signal and target genes. *Toxicol. Appl. Pharmacol.* 220: 320–332.
30. Martin, B., K. Hirota, D. J. Cua, B. Stockinger, and M. Veldhoen. 2009. Interleukin-17-producing γδ T cells selectively expand in response to pathogen products and environmental signals. *Immunity* 31: 321–330.
31. Cookson, W., M. Moffatt, and D. P. Strachan. 2011. Genetic risks and childhood-onset asthma. *J. Allergy Clin. Immunol.* 128: 266–270, quiz 271–272.
32. Dozor, A. J. 2010. The role of oxidative stress in the pathogenesis and treatment of asthma. *Ann. N. Y. Acad. Sci.* 1203: 133–137.
33. Nowak-Wegrzyn, A., and A. Fiocchi. 2010. Is oral immunotherapy the cure for food allergies? *Curr. Opin. Allergy Clin. Immunol.* 10: 214–219.
34. Al-Sabbagh, M., L. Fusi, J. Higham, Y. Lee, K. Lei, A. C. Hanyaloglu, E. W.-F. Lam, M. Christian, and J. J. Brosens. 2011. NADPH oxidase-derived reactive oxygen species mediate decidualization of human endometrial stromal cells in response to cyclic AMP signaling. *Endocrinology* 152: 730–740.
35. Henri, P., S. Beaumel, A. Guezennec, C. Poumès, P.-E. Stoebner, M.-J. Stasia, J. Guesnet, J. Martinez, and L. Meunier. 2011. MC1R expression in HaCaT keratinocytes inhibits UVA-induced ROS production via NADPH oxidase- and cAMP-dependent mechanisms. *J. Cell. Physiol.*
36. Irvin, B. J., C. L. Hanson, L. H. Smith, and C. K. Daniels. 2001. Cyclic AMP- and IL6-signaling cross talk: comodulation of proliferation and apoptosis in the 7TD1 B cell hybridoma. *Exp. Cell Res.* 265: 73–79.
37. Wang, P., F. Zhu, and K. Konstantopoulos. 2010. Prostaglandin E_2 induces interleukin-6 expression in human chondrocytes via cAMP/protein kinase A- and phosphatidylinositol 3-kinase-dependent NF-κB activation. *Am. J. Physiol. Cell Physiol.* 298: C1445–C1456.
38. Mortaz, E., G. Folkerts, and F. Redegeld. 2011. Mast cells and COPD. *Pulm. Pharmacol. Ther.* 24: 367–372.
39. de Boer, O. J., J. J. van der Meer, P. Teeling, C. M. van der Loos, M. M. Idu, F. van Maldegem, J. Aten, and A. C. van der Wal. 2010. Differential expression of interleukin-17 family cytokines in intact and complicated human atherosclerotic plaques. *J. Pathol.* 220: 499–508.
40. Noordenbos, T., N. Yeremenko, I. Gofita, M. van de Sande, P. P. Tak, J. D. Cañete, and D. Baeten. 2012. Interleukin-17-positive mast cells contribute to synovial inflammation in spondylarthritis. *Arthritis Rheum.* 64: 99–109.
41. Lakhdar, R., S. Denden, A. Kassab, N. Leban, J. Knani, G. Lefranc, A. Miled, J. B. Chibani, and A. H. Khelil. 2011. Update in chronic obstructive pulmonary disease: role of antioxidant and metabolizing gene polymorphisms. *Exp. Lung Res.* 37: 364–375.
42. Shen, N., J. Wang, M. Zhao, F. Pei, and B. He. 2011. Anti-interleukin-17 antibodies attenuate airway inflammation in tobacco-smoke-exposed mice. *Inhal. Toxicol.* 23: 212–218.
43. Chiba, T., H. Uchi, F. Yasukawa, and M. Furue. 2011. Role of the arylhydrocarbon receptor in lung disease. *Int. Arch. Allergy Immunol.* 155(Suppl. 1): 129–134.
44. Baglole, C. J., P. J. Sime, and R. P. Phipps. 2008. Cigarette smoke-induced expression of heme oxygenase-1 in human lung fibroblasts is regulated by intracellular glutathione. *Am. J. Physiol. Lung Cell. Mol. Physiol.* 295: L624–L636.
45. Kaminska, M., S. Foley, K. Maghni, C. Storness-Bliss, H. Coxson, H. Ghezzo, C. Lemière, R. Olivenstein, P. Ernst, Q. Hamid, and J. Martin. 2009. Airway remodeling in subjects with severe asthma with or without chronic persistent airflow obstruction. *J. Allergy Clin. Immunol.* 124: 45–51.e1-4.
46. Smith, M. J., and R. H. Garrett. 2005. A heretofore undisclosed crux of eosinophilia-myalgia syndrome: compromised histamine degradation. *Inflamm. Res.* 54: 435–450.

Downloaded from http://jimmunol.org/ at Inst Superiore de Sanita-Roma on June 4, 2012

Supplemental figure legends:

Supplemental Figure 1. (A) BMMC viability curve upon treatment with different concentration of FICZ. BMMCs were incubated 24-, 48-, 72-, and 96-h with increasing concentration of FICZ (300 nM, 600 nM and 900 nM) and viability was assessed by trypan blue staining. Graph shows means ± S.E.M. from two independent experiments. **(B) Characterization of AhR-deficient (AhR$^{-/-}$) BMMCs.** WT and AhR-deficient BMMCs (AhR$^{-/-}$) were tested for FcεRI (clone JRK, Rivera, J., J. P. Kinet, J. Kim, C. Pucillo, and H. Metzger. 1988. Studies with a monoclonal antibody to the beta subunit of the receptor with high affinity for immunoglobulin E. *Mol. Immunol.* 25: 647-61) expression by flow cytometry. **(C) Different timing of double FICZ stimulation on BMMCs degranulation.** IgE-sensitized WT BMMCs were untreated or treated with 300 nM FICZ for 16h+3h, 16h+4h, 24h+3h, 48h+3h before Ag addition. β-hexosaminidase was quantified 30 min upon Ag addition. Graphs are from two independent experiments.

Supplemental Figure 2. (A) IL-17 production in WT and AhR-deficient (AhR$^{-/-}$) BMMCs. 2x10^{6}/ml BMMCs WT (upper panels) and AhR-deficient BMMCs (AhR$^{-/-}$, lower panels) were incubated with 500 nM FICZ for 72 h and re-stimulated with 50 ng/ml PMA and 500 ng/ml ionomycin for 4h. Cell were fixed with Fix Buffer for 60 min at 4°C, washed with Perm Buffer and stained with anti IL-17A PerCP-Cy5.5 (all from eBiosciences, USA). Relative fluorescence intensities were quantified by flow cytometric analysis (FL-3 channel). Gates show percentages of IL-17-positive cells and mean fluorescence index (MFI). One of three representative experiments is shown. **(B) Quantitative PCR for *Rorc* gene. *Rorc* mRNA was evaluated** in anti-CD3 plus anti-CD28 activated CD4^{+} cells, unstimulated BMMCs, BMMCs stimulated with 300 nM FICZ for 4h and 24h. Murine primers for *Rorc* were used as in Kang, M.

A., J. Y. Beak, X. Wu, J. M. Gimble, T. Wada, W. Xie, J. B. Collins, S. F. Grissom, and A. M. Jetten. 2007. Gene expression profiling reveals a regulatory role for ROR alpha and ROR gamma in phase I and phase II metabolism. *Physiol. Genom*. 31: 281-94.

Results are expressed as fold induction over activated $CD4^+$ cells. Means ± S.E.M. from 3 independent experiments are shown. N.d., not detectable.

Supplemental Figure 1

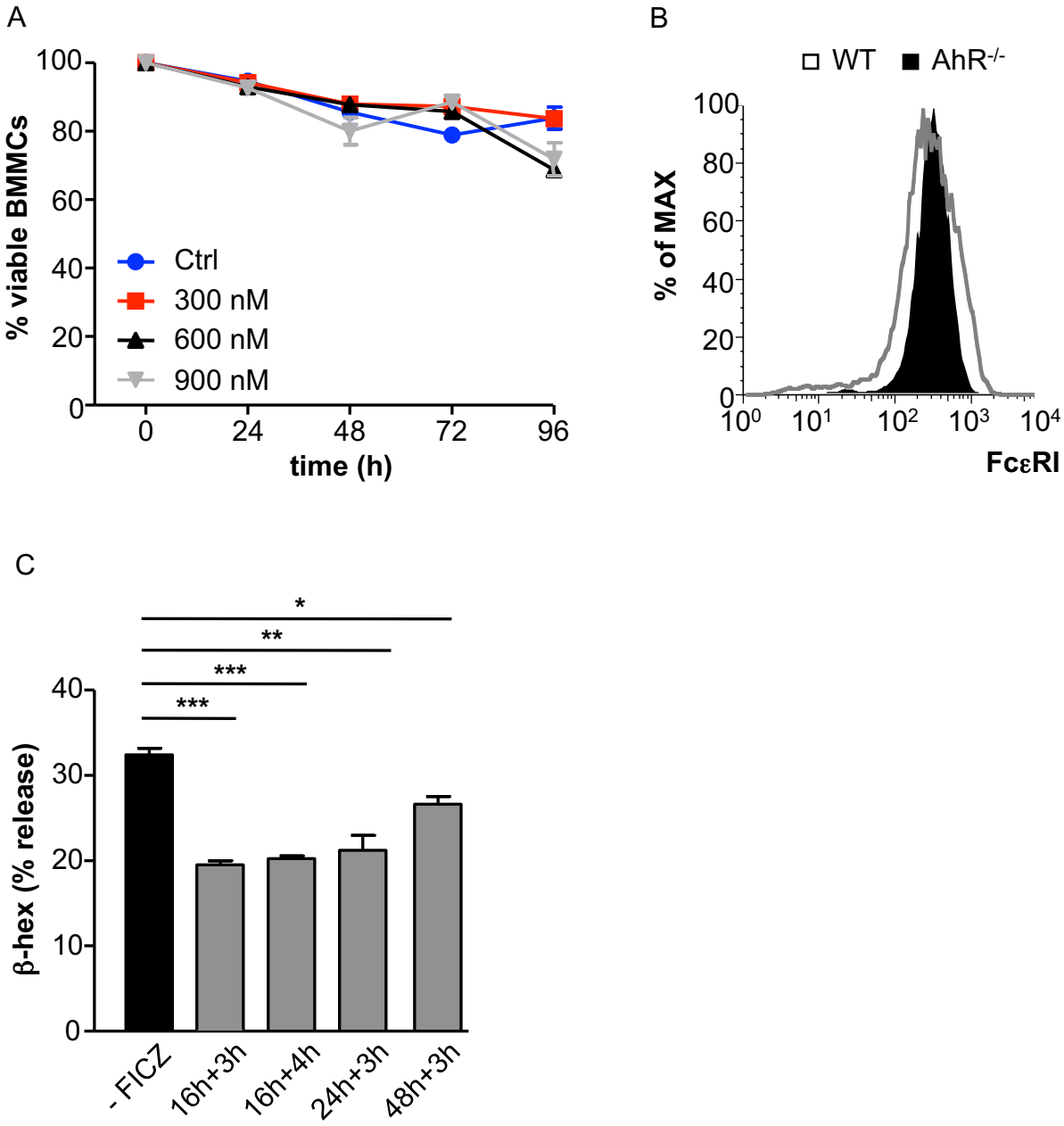
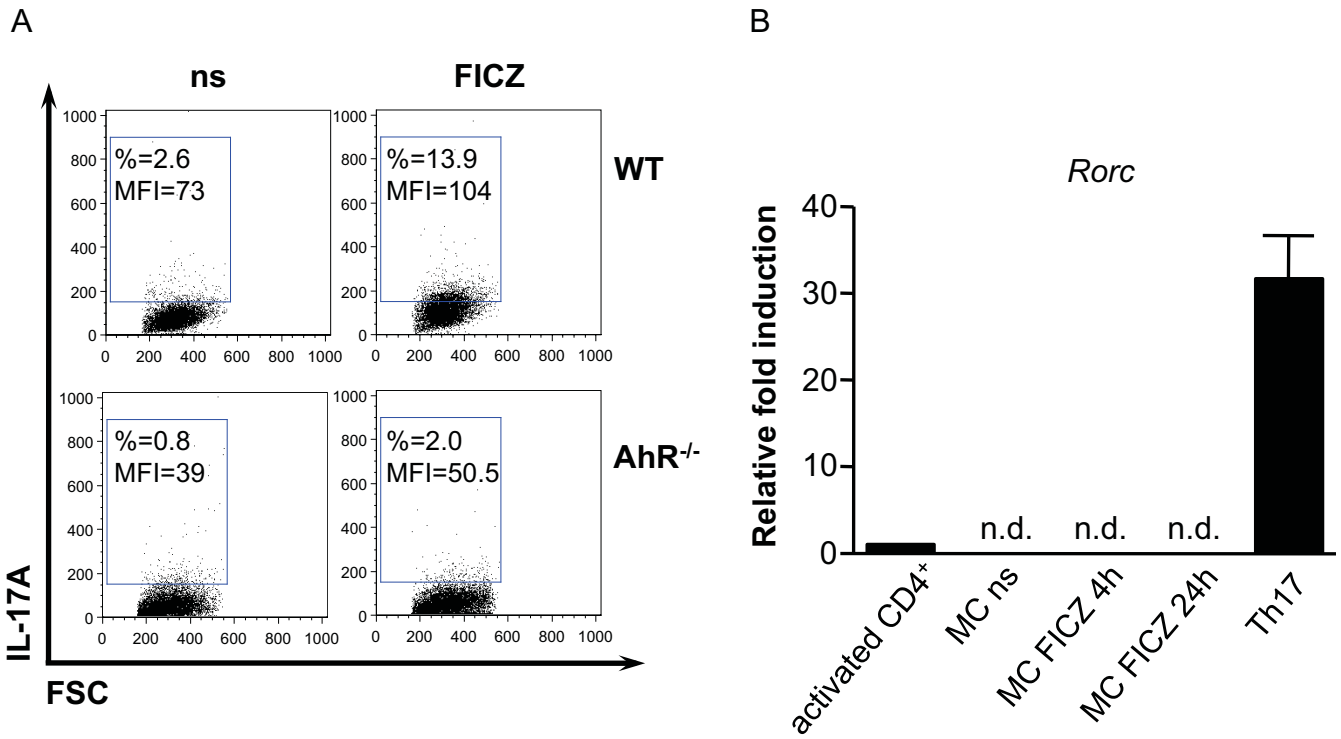
Supplemental Figure 2